Spin splitting in bulk wurtzite AlN under biaxial strain

Hsiu-Fen Kao, Ikai Lo, Jih-Chen Chiang, Meng-En Lee, C. L. Wu, W. T. Wang, Chun-Nan Chen, and Y. C. Hsu

Citation: Journal of Applied Physics **111**, 103716 (2012); doi: 10.1063/1.4720469
View online: http://dx.doi.org/10.1063/1.4720469
View Table of Contents: http://scitation.aip.org/content/aip/journal/jap/111/10?ver=pdfcov
Published by the AIP Publishing

Spin splitting in bulk wurtzite AlN under biaxial strain

Hsiu-Fen Kao,[1,2,a)] Ikai Lo,[1,a)] Jih-Chen Chiang,[1] Meng-En Lee,[3] C. L. Wu,[1] W. T. Wang,[1] Chun-Nan Chen,[4] and Y. C. Hsu[1]
[1]*Department of Physics, Center for Nanoscience and Nanotechnology, National Sun Yat-sen University, Kaohsiung 80424, Taiwan*
[2]*Institute of Photonics and Communications, National Kaohsiung University of Applied Sciences, Kaohsiung 80778, Taiwan*
[3]*Department of Physics, National Kaohsiung Normal University, Yanchao, Kaohsiung 82444, Taiwan*
[4]*Department of Physics, Tamkang University, Tamsui, New Taipei City 25137, Taiwan*

(Received 3 January 2012; accepted 23 April 2012; published online 25 May 2012)

The spin-splitting energies in biaxially strained bulk wurtzite material AlN are calculated using the linear combination of atomic orbital (LCAO) method, and the equi-spin-splitting distributions in k-space near the minimum-spin-splitting (MSS) surfaces are illustrated. These data are compared with those derived analytically by two-band $\mathbf{k}\cdot\mathbf{p}$ (2KP) model. It is found that the results from these two methods are in good agreement for small k. However, the ellipsoidal MSS surface under biaxial compressive strain does not exist in the 2KP model, because the data points are far from the Γ point. Instead, three basic shapes of the MSS surface occur in the wurtzite Brillouin zone: a hyperboloid of two sheets, a hexagonal cone, and a hyperboloid of one sheet, evaluated from the LCAO method across the range of biaxial strains from compressive to tensile. © *2012 American Institute of Physics*. [http://dx.doi.org/10.1063/1.4720469]

I. INTRODUCTION

Spintronics has received considerable attention in the field of semiconductor research in recent years. Several types of transistors utilizing spin properties of semiconductors have been proposed.[1–3] One of these proposed spin devices, the resonant spin lifetime (RSL) transistor, is based on the special properties of the spin lifetime tensor arising from the interplay between bulk inversion asymmetry (BIA) and structure inversion asymmetry (SIA) in zinc-blende[4] or wurtzite[5] quantum wells (QWs). In zinc-blende semiconductors, unstrained BIA yields a cubic-k term (called the Dresselhaus effect),[6] while strain[7,8] and SIA lead to a linear-k term (named the Rashba effect)[9] in the two-band $\mathbf{k}\cdot\mathbf{p}$ (2KP) Hamiltonian. In bulk wurtzite semiconductors, there are also two types of wurtzite bulk inversion asymmetry (WBIA) effects.[5,10–13] In the nearest-neighbor linear combination of atomic orbitals (LCAO) model, the ideal wurtzite structure yields only the type-II WBIA effect (called the Dresselhaus effect in Ref. 10), while deviations from the ideal structure caused by the crystal field or strain yield the type-I WBIA effect (called the Rashba effect in Ref. 11). The type-II WBIA effect induces a cone-shaped minimum-spin-splitting (MSS) surface in the ideal wurtzite Brillouin zone. Since the spin splitting on the MSS surface is generally very weak, it can be regarded as a spin-degenerate surface.[10] When the crystal field and strain are taken into account, the type-I WBIA effect induces a shape-controllable MSS surface (i.e., a MSS surface that can become a hyperboloid of two sheets, a hexagonal cone, or a hyperboloid of one sheet) in the real wurtzite Brillouin zone. Such a shape-controllable MSS surface also makes the wurtzite material a potential candidate for spintronic devices.[5,10,11] Based on the mechanics of spin-orbit interaction, the interplay between Rashba and Dresselhaus effects will determine the shape of MSS surface of wurtzite aluminum nitride (AlN), which is crucial information in the band-engineering of AlN-based materials for spintronic application. Consequently, the role of biaxial strain and its influence on the MSS surface have to be solved when one wants to engineer the AlN-based materials for spintronic devices.

However, the shape of the MSS surface still has not been studied under biaxial compressive strain. It requires a better understanding of the change of spin-splitting energies near the MSS surface in order to design spintronic devices, such as the RSL transistor. Therefore, it is important to study the equi-spin-splitting (ESS) distribution near the MSS surface, as well. However, the ESS distribution near the MSS surface under different strains is still unknown. In this paper, we shall investigate from biaxial compressive to biaxial tensile strains on the shapes of the MSS surfaces and the ESS distribution near these MSS surfaces by using the LCAO method, and compare these results to those obtained with the 2KP model. We show that the MSS and ESS surfaces calculated by the 2KP model are in good agreement with LCAO calculations for small k, but inconsistent for large k. It is also shown that the ellipsoidal MSS surface predicted by the 2KP model under biaxial compressive strain does not exist, because the MSS data points are far from the Γ point in this case.

II. METHODS AND RESULTS

To calculate the spin-splitting energies in bulk wurtzite materials, the band structures for both unstrained and biaxially strained wurtzite AlN are computed using the sp^3 LCAO method with spin-orbit coupling. The Hamiltonian $H(\vec{k})$ can be written in the form,

a)Authors to whom correspondence should be addressed. Electronic addresses: fenny@cc.kuas.edu.tw and ikailo@mail.phys.nsysu.edu.tw.

$$H(\vec{k}) = H_0(\vec{k}) + H_{SO} = \begin{bmatrix} H_0^{\uparrow\uparrow}(\vec{k}) & 0 \\ 0 & H_0^{\downarrow\downarrow}(\vec{k}) \end{bmatrix} + \begin{bmatrix} H_{SO}^{\uparrow\uparrow} & H_{SO}^{\uparrow\downarrow} \\ H_{SO}^{\downarrow\uparrow} & H_{SO}^{\downarrow\downarrow} \end{bmatrix}, \quad (1)$$

where $H_0^{\alpha\alpha}(\vec{k})$ is the Hamiltonian without the spin-orbit terms ($\alpha = \uparrow$ or $\downarrow$), where $\vec{k} = \vec{k}_{//} + \hat{z}k_z = k_{//}(\hat{x}\cos\theta + \hat{y}\sin\theta) + \hat{z}k_z$, $\vec{k}_x // \overrightarrow{\Gamma M}$, and $\vec{k}_y // \overrightarrow{\Gamma K}$. The renormalized spin-orbit splitting of the anion and cation p states (e.g., $\Delta_N = 9$ meV and $\Delta_{Al} = 24$ meV) in $H_{SO}^{\alpha\beta}$ ($\alpha, \beta = \uparrow$ or $\downarrow$) is given in Refs. 14 and 15. The LCAO parameters are listed in Table I of Ref. 16. When the crystal field is taken into account, the band structure of the unstrained wurtzite material is obtained by differentiating the bond in the [001] direction from the three other bonds.[17] The corresponding LCAO parameters used in these strained cases are obtained through Harrison's d^{-2} rule[18–20] and modification of the Slater-Koster coefficients[21] from those of the ideal wurtzite structure.[16] The spin-splitting energies of the lowest conduction band are obtained from the eigenvalues of the above Hamiltonian $H(\vec{k})$.

In the 2KP Hamiltonian, the spin-orbit component induced by the type-II WBIA effect is $H_{SO}^0(\vec{k}) = (-\gamma_0 k_{//}^2 + \lambda_0 k_z^2)(\sigma_x k_y - \sigma_y k_x)$, where γ_0 and λ_0 are the type-II WBIA coefficients, and $\lambda_0/\gamma_0 \approx 4$.[10] As the crystal field and biaxial strain[22] are taken into account, a perturbation term $H'_{SO}(\vec{k}) = (\alpha_{wz} - \gamma' k_{//}^2 + \lambda' k_z^2)(\sigma_x k_y - \sigma_y k_x)$ induced by the type-I WBIA effect is added to the spin-orbit component, where α_{wz}, γ', and λ' are the type-I WBIA coefficients.[9–11,23] As a result, the spin-orbit component of the 2KP Hamiltonian can be written as $H_{SO}(\vec{k}) = H_{SO}^0 + H'_{SO} = (\alpha_{wz} - \gamma_{wz} k_{//}^2 + \lambda_{wz} k_z^2)(\sigma_x k_y - \sigma_y k_x)$, where α_{wz}, γ_{wz}, and λ_{wz} are the WBIA coefficients, as well as the 2KP parameters. Here, $\gamma_{wz} = \gamma_0 + \gamma'$ and $\lambda_{wz} = \lambda_0 + \lambda'$.[10,11] The spin-splitting energy (δE) can be, therefore, described by[10,11]

$$\delta E = 2k_{//}(\alpha_{wz} - \gamma_{wz} k_{//}^2 + \lambda_{wz} k_z^2). \quad (2)$$

To calculate the MSS and ESS surfaces in k-space analytically using the 2KP model, we write Eq. (2) as $2\gamma_{wz} k_{//}^3 - 2(\alpha_{wz} + \lambda_{wz} k_z^2) k_{//} + \delta E = 0$. Therefore, by calculating k_z for the MSS and ESS surfaces, the analytical solution as a function of $k_{//}$ with the 2KP model can be written as

$$k_z = \pm \frac{\sqrt{-\delta E + 2\alpha_{wz} k_{//} - 2\gamma_{wz} k_{//}^3}}{\sqrt{-2\lambda_{wz} k_{//}}}. \quad (3)$$

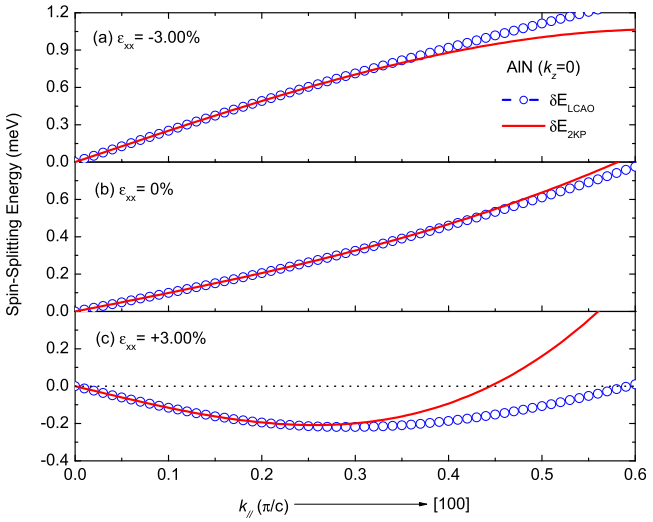

FIG. 1. Spin splitting as a function of $k_{//}$ under various external strains with $k_z = 0$ (π/c) in bulk wurtzite AlN for (a) a biaxially strained wurtzite structure with $\varepsilon_{xx} = -3.00\%$, (b) the unstrained wurtzite structure with $\varepsilon_{xx} = 0\%$, and (c) a biaxially strained wurtzite structure with $\varepsilon_{xx} = 3.00\%$. These results were calculated by using the LCAO and 2KP methods.

k_z must be real, therefore, according to this formula, $(-\delta E + 2\alpha_{wz} k_{//} - 2\gamma_{wz} k_{//}^3) \geq 0$, since $\lambda_{wz} < 0$ (see Table I). For small $k_{//}$, where $\frac{1}{k_{//}} >> k_{//}^2$, the term containing $\sqrt{\frac{\delta E}{2\lambda_{wz} k_{//}}}$ in Eq. (3) dominates, and k_z is proportional to $\pm\frac{1}{\sqrt{k_{//}}}$. It is predicted that a sharp rise in k_z takes place in the range of small $k_{//}$ for the ESS surfaces. Conversely, for large $k_{//}$, where $\frac{1}{k_{//}} \ll k_{//}^2$, the term containing $\sqrt{\frac{\gamma_{wz} k_{//}^2}{\lambda_{wz}}}$ in Eq. (3) dominates, and k_z is proportional to $\pm k_{//}$. It is, therefore, predicted that the ESS surface yields a linear behavior for large $k_{//}$. Here, the value of $\frac{\alpha_{wz}}{\lambda_{wz}}$ is very small (see Table I), and thus it can be ignored.

To study the ESS distributions near the MSS surfaces in bulk wurtzite materials, we show results for bulk AlN as examples. First, we compare the spin splitting calculated by the LCAO and the 2KP methods over the range of biaxial strains[22] from compressive through tensile, as shown in Fig. 1. Second, we illustrate the ESS distribution near the MSS surface under different biaxial strains by using the LCAO method, as shown in Fig. 2. Finally, a comparison of the ESS and the MSS surfaces under different biaxial strains calculated by both the 2KP model and the LCAO method is shown in Fig. 3. In our calculation, the 2KP parameters used

TABLE I. The 2KP parameters under different strains for wurtzite AlN used in this paper.

Strain%	$\varepsilon_{xx} = -3.00\%$	$\varepsilon_{xx} = 0\%$	$\varepsilon_{xx} = +1.43\%$	$\varepsilon_{xx} = +3.00\%$
2KP parameters	$\alpha_{wz} = 2.02455$	$\alpha_{wz} = 0.77011$	$\alpha_{wz} = 0.00720$	$\alpha_{wz} = -0.93568$
	(meV · Å)	(meV · Å)	(meV · Å)	(meV · Å)
	$\gamma_{wz} = 4.31701$	$\gamma_{wz} = -2.25910$	$\gamma_{wz} = -6.22200$	$\gamma_{wz} = -11.18130$
	(meV · Å^3)	(meV · Å^3)	(meV · Å^3)	(meV · Å^3)
	$\lambda_{wz} = -37.57961$	$\lambda_{wz} = -28.40268$	$\lambda_{wz} = -23.11324$	$\lambda_{wz} = -16.44389$
	(meV · Å^3)	(meV · Å^3)	(meV · Å^3)	(meV · Å^3)

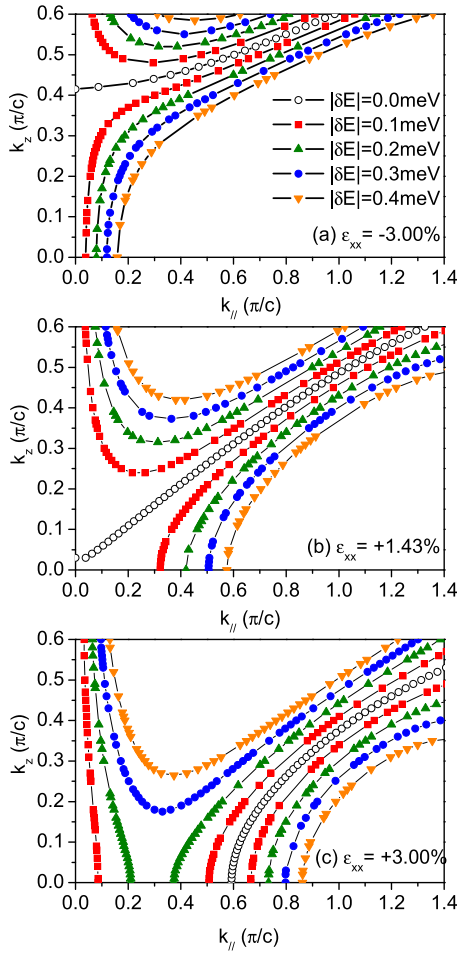

FIG. 2. The ESS distribution near the MSS surface as a function of $k_{//}$under various external strains in bulk wurtzite AlN for (a) biaxial strain with $\varepsilon_{xx} = -3.00\%$, (b) biaxial strain with $\varepsilon_{xx} = 1.43\%$, and (c) biaxial strain with $\varepsilon_{xx} = 3.00\%$, as calculated for various values of k_z, using the LCAO method.

for wurtzite AlN under different strain are obtained by fitting the spin-splitting energy data from the LCAO method and are listed in Table I. The signs of the 2KP parameters and the shapes of the MSS surfaces are calculated by the 2KP and LCAO methods for three ranges of biaxial strains from compressive to tensile, as listed in Table II. The extension of the 2KP parameters as functions of external strains obtained from our previous research, which can be referred from Ref. 11.

Figure 1 shows the spin splitting as a function of $k_{//}$ under various external strains ($\varepsilon_{xx} = -3.00\%$, 0%, and 3.00%) with $k_z = 0$ (π/c). Here, ε_{xx} denotes the biaxial strain tensor component, i.e., $\varepsilon_{xx} = \varepsilon_{yy} = (a - a_0)/a_0$.[22] a and a_0 denote the strained and unstrained lattice constants in the wurtzite structure, respectively. The open circles are obtained from the nearest-neighbor LCAO method, and the solid lines are the results of fitting to the 2KP model. As can be seen, the results from the two-band model are in good agreement with those from the LCAO method for $k_{//} < 0.3$ (π/c). Therefore, the 2KP parameters evaluated from it are utilized for investigating the ESS surface near the MSS surface under various external strains in bulk wurtzite materials in the range of small k. For the compressively strained ($\varepsilon_{xx} = -3.00\%$) and unstrained ($\varepsilon_{xx} = 0\%$) wurtzite materials, the spin splitting calculated using the LCAO method exhibits a linear behavior [see Figs. 1(a) and 1(b)]. These results imply that the type-I WBIA effect dominates the spin splitting in both compressively strained and unstrained wurtzite materials, due to the dominance of the linear-k term. For the tensilely strained ($\varepsilon_{xx} = 3.00\%$) wurtzite structure, a spin-degenerate surface exists on the $k_z = 0.0$ (π/c) plane in the wurtzite Brillouin zone [see Fig. 1(c)]. This is because in this case, the interplay between the linear-$k_{//}$ and cubic-$k_{//}$ terms generates spin-degenerate points in the plane of $k_z = 0.0$ (π/c) in the tensilely strained wurtzites.[11] In the compressive strain, for large $k_{//}$, the spin splitting predicted by the 2KP model is decreasing and smaller than that using by the LCAO method. Conversely, in the tensile strain, for large $k_{//}$, the spin splitting predicted by the 2KP model is much larger than that using by the LCAO method. Note that for unstrained wurtzite, the 2KP model gives results that are valid over a wide range of the Brillouin zone. For strained wurtzite, the results predicted by the 2KP model are valid near the zone center ($k_{//} < 0.3\,\pi$/c), but are not valid far from the Γ point.

Figure 2 shows the ESS distribution near the MSS surface in bulk wurtzite AlN under various external strains, as calculated with the LCAO method. For a biaxially strained wurtzite material with $\varepsilon_{xx} = -3.00\%$ or $\varepsilon_{xx} = 1.43\%$, it can be seen that the shape of the MSS surface is a hyperboloid of two sheets or a hexagonal cone, respectively. The shapes of the ESS distribution near these MSS surfaces have two basic forms: a hyperboloid of one sheet, and an approximate, asymmetric hyperboloid surface [see Figs. 2(a) and 2(b)]. For a biaxially strained wurtzite material with $\varepsilon_{xx} = 3.00\%$, it is seen that the shape of the MSS surface is a hyperboloid of one sheet. The shapes of the ESS distribution near this MSS surface have three types: a hyperboloid of one sheet, an approximate, asymmetric hyperboloid surface, and an opposing hyperboloid of one sheet [see Fig. 2(c)]. When $k_{//} = 0$, the high symmetry of the bulk material results in zero spin-splitting energy (spin degeneracy) along the [001] direction, due to time-reversal symmetry. Note that one type of the ESS distribution is an approximate, asymmetric hyperboloid surface not only near the MSS surface but also near this spin-degenerate line (when $k_{//} = 0$).

Figure 3 shows the ESS surface near the MSS surface under different biaxial strains, as calculated by using both the 2KP model and the LCAO method. For a biaxially strained wurtzite structure with $\varepsilon_{xx} = -3.00\%$, the shape of the ESS ($\delta E = 0.1$ meV) surface calculated by the 2KP model can be seen to be in good agreement with that calculated by the LCAO method for small k ($k_{//} < 0.05\,\pi$/c and $k_z < 0.2\,\pi$/c). For large k, the shape of the MSS ($\delta E = 0.0$ meV) surface calculated by the 2KP model is ellipsoidal and is inconsistent with that calculated by the LCAO method [see Fig. 3(a)]. We note that the ellipsoidal MSS surface under biaxial compressive strain predicted by the 2KP model does not exist, since the MSS data points in this case are far from the Γ point. We also note that the 2KP model predicts that a sharp rise in k_z takes place in the range of small $k_{//}$ on the ESS surfaces; this result is consistent with that calculated by the LCAO method. For the unstrained wurtzite material with $\varepsilon_{xx} = 0\%$, it is seen that the shape of the ESS ($\delta E = 0.1$ meV) surface calculated

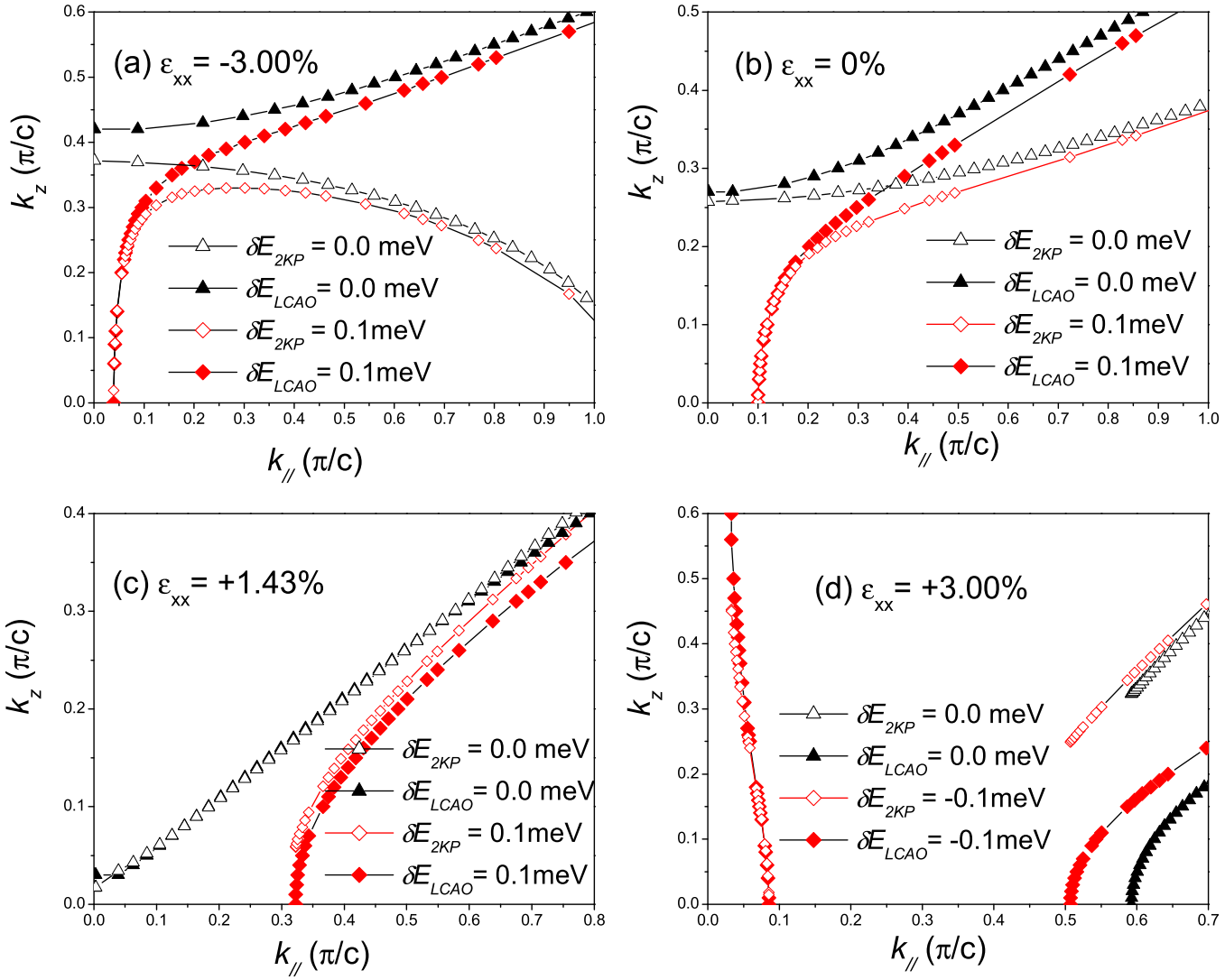

FIG. 3. The MSS and ESS curves as a function of $k_{//}$under various external strains in bulk wurtzite AlN for (a) biaxially strain with $\varepsilon_{xx} = -3.00\%$ for $\delta E = 0.0$ and 0.1 meV, (b) the unstrained wurtzite structure with $\varepsilon_{xx} = 0\%$ for $\delta E = 0.0$ and 0.1 meV, (c) biaxial strain with $\varepsilon_{xx} = 1.43\%$ in $\delta E = 0.0$ and 0.1 meV, (d) biaxial strain with $\varepsilon_{xx} = 3.00\%$ for $\delta E = 0.0$ and -0.1 meV, as calculated for various values of k_z using the 2KP and LCAO methods.

by the 2KP model is a hyperboloid of one sheet and is in good agreement with that calculated by the LCAO method for small k ($k_{//}$ and $k_z < 0.15\,\pi/c$). Also, the shape of the MSS ($\delta E = 0.0$ meV) surface calculated by the 2KP model is a hyperboloid of two sheets and agrees with that calculated by the LCAO method [see Fig. 3(b)]. On the ESS surface, the change of k_z is dramatically large in the range of small $k_{//}$, but shows a linear behavior for large $k_{//}$ that is predicted by the 2KP model, consistent with the result calculated by the LCAO method. For a biaxially strained wurtzite material with $\varepsilon_{xx} = 1.43\%$, the shape of the MSS ($\delta E = 0.0$ meV) surface calculated by the 2KP model is a hexagonal cone and is in good agreement with that calculated by the LCAO method. The shape of the ESS ($\delta E = 0.1$ meV) surface calculated by the 2KP model is a hyperboloid of one sheet and agrees with that calculated by the LCAO method. However, for

TABLE II. The signs of the 2KP parameters and the shapes of the MSS surface predicted by the 2KP and LCAO methods under different strains for wurtzite AlN.

Strain%	$-5.00\% \le \varepsilon_{xx} \le -1.00\%$	$-1.00\% < \varepsilon_{xx} \le +1.43\%$	$+1.43\% < \varepsilon_{xx} \le +5.00\%$
2KP parameters	$\alpha_{wz} > 0$	$\alpha_{wz} > 0$	$\alpha_{wz} < 0$
	$\gamma_{wz} > 0$	$\gamma_{wz} < 0$	$\gamma_{wz} < 0$
	$\lambda_{wz} < 0$	$\lambda_{wz} < 0$	$\lambda_{wz} < 0$
	$\alpha_{wz}/\gamma_{wz} > 0$	$\alpha_{wz}/\gamma_{wz} < 0$	$\alpha_{wz}/\gamma_{wz} > 0$
	$\alpha_{wz}/\lambda_{wz} < 0$	$\alpha_{wz}/\lambda_{wz} < 0$	$\alpha_{wz}/\lambda_{wz} > 0$
Shape of MSS surface predicted by 2KP	ellipsoid	a hyperboloid of two sheets	a hyperboloid of one sheet
Shape of MSS surface predicted by LCAO	a hyperboloid of two sheets	a hyperboloid of two sheets	a hyperboloid of one sheet

$k_{//} < 0.32\,\pi/c$, the ESS data points ($\delta E = 0.1$ meV) predicted by the 2KP model do not exist, due to the lack of an analytical solution for k_z when $(-\delta E + 2\alpha_{wz}k_{//} - 2\gamma_{wz}k_{//}^3) < 0$ [see Fig. 3(c)]. For a biaxially strained wurtzite with $\varepsilon_{xx} = 3.00\%$, for $k_{//} < 0.1\,\pi/c$, the shape of the ESS ($\delta E = -0.1$ meV) surface calculated by the 2KP model is an opposing hyperboloid of one sheet and is in good agreement with that calculated by the LCAO method for $k_z < 0.25\,\pi/c$. However, the shape of the MSS ($\delta E = 0.0$ meV) surface calculated by the 2KP model disagrees with that calculated by the LCAO method, since the MSS data points in this case are far from the Γ point. In this case, the MSS (ESS) surface for $0.1\pi/c < k_{//} < 0.5\,\pi/c$ predicted by the 2KP model does not exist, due to the lack of an analytical solution for k_z when $(-\delta E + 2\alpha_{wz}k_{//} - 2\gamma_{wz}k_{//}^3) < 0$ [see Fig. 3(d)]. These results show that over the range of biaxial strains, from tensile to compressive, the spin splitting in wurtzite structures can be well described by the 2KP model near the zone center.

III. CONCLUSIONS

We have determined the ESS distribution near the MSS surface of wurtzite AlN under different biaxial strains by using the LCAO method and have compared them with those calculated by using the 2KP model. LCAO calculations in the wurtzite Brillouin zone show that the MSS surface can be described, over the range of biaxial strains from tensile to compressive, by just three basic shapes: a hyperboloid of two sheets, a hexagonal cone, and a hyperboloid of one sheet. It is also found that under biaxial compressive strain, the ellipsoidal MSS surface predicted by the 2KP model does not exist, as the MSS data points are far from the Γ point in this case. Moreover, we have demonstrated that the MSS and ESS surfaces calculated by the 2KP model with an analytical formula are in good agreement with LCAO calculations for small k, but disagree with LCAO calculations for large k. Specifically, the analytical solution of the 2KP model can identify the interplay between the types-I and II WBIA effects, investigate the ESS and the MSS surfaces, and accurately determine the spin splitting near the zone center in wurtzite structures. Therefore, the 2KP model is still valid and effective for the study of spintronics in wurtzite semiconductors.

ACKNOWLEDGMENTS

This project is supported by the National Science Council of Taiwan.

[1]S. Datta and B. Das, Appl. Phys. Lett. **56**, 665 (1990).
[2]J. Schliemann, J. C. Egues, and D. Loss, Phys. Rev. Lett. **90**, 146801 (2003).
[3]X. Cartoixà, D. Z. -Y.Z.-Y. Ting, and Y.-C. Chang, Appl. Phys. Lett. **83**, 1462 (2003).
[4]X. Cartoixà, D. Z. -Y.Z.-Y. Ting, and Y.-C. Chang, Phys. Rev. B **71**, 45313 (2005).
[5]W. T. Wang, C. L. Wu, J. C. Chiang, I. Lo, H. F. Kao, Y. C. Hsu, W. Y. Pang, D. J. Jang, M. E. Lee, Y. C. Chang, and C. N. Chen, J. Appl. Phys. **108**, 083718 (2010).
[6]G. Dresselhaus, Phys. Rev. **100**, 580 (1955); E. I. Rashba and V. I. Sheka, Sov. Phys. Solid State **3**, 1257 (1961).
[7]S. A. Crooker and D. L. Smith, Phys. Rev. Lett. **94**, 236601 (2005).
[8]G. L. Bir and G. E. Pikus, *Symmetry and Strain-Induced Effects in Semiconductors* (Halstead, New York, 1974).
[9]E. I. Rashba, Sov. Phys. Solid State **2**, 1109 (1960); Yu. A. Bychkov and E. I. Rashba, J. Phys. C **17**, 6039 (1984).
[10]W. T. Wang, C. L. Wu, S. F. Tsay, M. H. Gau, I. Lo, H. F. Kao, D. J. Jang, J. C. Chiang, M. E. Lee, Y. C. Chang, C. N. Chen, and H. C. Hsueh, Appl. Phys. Lett. **91**, 082110 (2007).
[11]C. L. Wu, S. F. Tsay, W. T. Wang, M. H. Gau, J. C. Chiang, I. Lo, H. F. Kao, Y. C. Hsu, D. J. Jang, M. E. Lee, and C. N. Chen, J. Phys. Soc. Jpn., Part 1 **79**, 093705 (2010).
[12]I. Lo, W. T. Wang, M. H. Gau, S. F. Tsay, and J. C. Chiang, Phys. Rev. B **72**, 245329 (2005).
[13]L. C. L. Y. Voon, M. Willatzen, M. Cardona, and N. E. Christensen, Phys. Rev. B **53**, 10703 (1996), and references therein.
[14]D. J. Chadi, Phys. Rev. B **16**, 790 (1977).
[15]J. C. Phillips, *Bonds and Bands in Semiconductors* (Academic, San Diego, CA, 1973), p. 179.
[16]A. Kobayashi, O. F. Sankey, S. M. Volz, and J. D. Dow, Phys. Rev. B **28**, 935 (1983).
[17]A. Niwa, T. Ohtoshi, and T. Kuroda, Appl. Phys. Lett. **70**, 2159 (1997).
[18]W. A. Harrison, Phys. Rev. B **14**, 702 (1976).
[19]W. A. Harrison and S. T. Pantilides, Phys. Rev. B **14**, 691 (1976).
[20]W. A. Harrison, *Electronic Structure and the Properties of Solids* (Dover, New York, 1989).
[21]J. C. Slater and G. F. Koster, Phys. Rev. **94**, 1498 (1954).
[22]J.-M. Wagner and F. Bechstedt, Phys. Rev. B **66**, 115202 (2002).
[23]K. Tsubaki, N. Maeda, T. Saitoh, and N. Kobayashi, Appl. Phys. Lett. **80**, 3126 (2002).